Hydraulic and Civil Engineering Technology VII
M. Yang et al. (Eds.)

doi:10.3233/ATDE220917

Analysis of Ultimate Bearing Capacity of Prefabricated Airport Pavement Panel

Peng DING [a,1], Zhiguo LIU [a], Menglin LI [b], Ran ZHOU [c], Wenzhan JI [a] and Mengmeng ZHANG [a]
[a] *China Construction Science & Technology Group Co., Ltd, Beijing 100195, China*
[b] *Zhongke Shian Technology Co., Ltd, Beijing 100142, China*
[c] *Beijing Railway Construction Co., Ltd., China Railway Sixth Engineering Bureau Group, Beijing 100036, China*

Abstract. In order to study the bearing performance of the new prefabricated airport pavement panel (PAPP) structure, a three-dimensional finite element model (3D-FEM) of "square PAPP - stratum" was established based on ABAQUS finite element analysis platform, and then the mechanical and deformation performance analysis under single wheel various limit load positions was carried out. The research showed that the influence radius was less than the side length R of the panel, The maximum opening or minimum compression of the joint under single wheel conditions was very small, and the maximum principal stress value of the precast concrete panel was an important key control factor for the ultimate load-bearing capacity. Under the action of vertical load, the tenon and groove joint connects multiple independent prefabricated panels to form a whole through mutual occlusal action. The research work provided a useful reference for the design and construction of PAPP.

Keywords. Prefabricated, airport pavement panel, ultimate bearing, 3D-FEM, tenon and groove joint

1. Introduction

Airport runway panel is an important structural carrier to ensure the safe take-off and landing of aircraft, in many application scenarios such as emergency rescue, military war, non-stop construction of airport roads, and rapid repair, more advanced technical process methods and shorter construction time are put forward for the rapid construction (repair) of airport road panels. Compared with the traditional cast-in-place structure construction process, the fabricated structure construction process has many advantages, such as industrialized, high-quality production, rapid on-site assembly, less wet operation, production and construction are not affected by weather and season, little impact on the social environment, short construction period and less maintenance in the later stage.

There are relatively few typical projects that use prefabricated technology for construction or testing in airport road engineering. The former Soviet Union took prefabricated panels and prestressed technology to build the airport runway [1]. Japan

[1] Peng Ding, Corresponding author, China Construction Science & Technology Group Co., Ltd, Beijing 100195, China; E-mail: dingpeng20@tsinghua.org.cn.

used prefabricated panel technology to build airport runways and popularized this technology to the terminal container yard [2]. The U.S. military has conducted many tests to quickly repair the damaged airport pavement by using prefabricated panel technology, and has obtained a series of test results and application experience [3-5]. At the end of 1990s, some commercial airports in North America tried to repair some airport runways with prefabricated panel technology and achieved good application: St. Louis Lambert International Airport [6], Washington Dulles International Airport [7-8], LaGuardia International Airport [9], Dallas – Fort Worth International Airport [10] and Vancouver International Airport [11]. Compared with foreign research, domestic research on prefabricated airport runway is still at the initial stage [12-14].

Based on ABAQUS finite element analysis platform, this paper establishes a three-dimensional finite element model (3D-FEM) of a new type of "square PAPP-stratum", and conducts comparative research on the key indicators such as mechanics, deformation and joint change of prefabricated panel structure under the action of single wheel load at the limit load level under multiple cases. The study hopes to provide scientific basis and engineering references for the design and construction of PAPP.

2. 3D-FEM

The pavement panel structure includes reinforced concrete precast panel, tenon and groove joint, panel rebar, prestressed rebar, etc. The panel to panel is connected with tenon and groove structure. The precast panel concrete is C40, and the upper and lower layers are arranged in the panel φ 12 distributed rebar, three reserved in the vertical and horizontal directions φ 20 prestressed rebar ducts shall be pre tensioned by post tensioning method during construction. The prestressed PAPP structure is shown in figure 1.

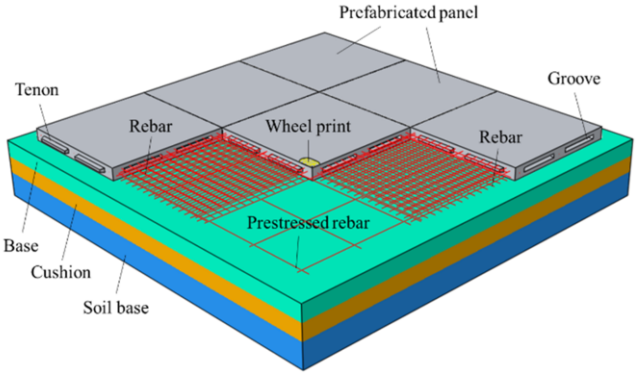

Figure 1. Prestressed PPAP structure.

A 3D-FEM of "square PPCP- stratum" is established as shown in figure 2. The stratum is divided into soil base layer, cushion layer and base layer from bottom to top. There are nine square assembled panels in total. The prefabricated panels are assembled by the combination of tenon and groove butt joint and prestressed rebar connection. The square panel and prefabricated panel base contact parts are set with contact surfaces to simulate the interaction and the Coulomb friction constitutive is

adopted for the contact surface. The prestressed rebar and the rebar in the panel are simulated by placing the embedded function in the concrete. In order to study the ultimate load condition of the model, the prestressed rebar is considered as the long-term prestressed loss to zero, i.e., no prestressed is favorable to the design. Since plastic damage is not allowed in normal operation of the airport road panel, elastic constitutive model is adopted for reinforced concrete panel model, solid element simulation is adopted for concrete panel and stratum.

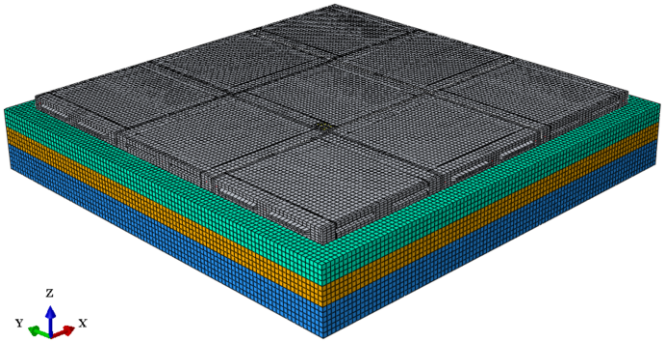

Figure 2. 3D-FEM of "square PAPP-stratum".

Material properties as shown in table 1. The four sides of the model stratum are 0.5 m larger than the outer sides of the nine prefabricated panels.

Table 1. Material properties of FEM.

Name	Material	Density (kg/m^3)	Young's modulus (GPa)	Poisson's ratio	Diameter / Thickness (mm)
Concrect	C40	2500	32.5	0.15	-
Prestressed rebar	HRB335	7500	206	0.25	φ20
Rebar in panel	HRB335	7500	206	0.25	φ12
Base	Cement stabilized materials	1900	6	0.20	400
Cashion	Graded crushed stone	1950	0.3	0.30	400
Soil base	Clay / silt	2010	0.1	0.35	600

According to the Specifications for Airport Cement Concrete Pavement Design of China (MH / T5004-2010), Boeing B-737-900 is selected as the model load analysis model, and the tire pressure of the main landing gear is 1.47 MPa, the length of the wheel printing is $L_t \approx 495$ mm, and the width of the wheel printing is $W_t \approx 297$ mm. The critical load position conditions of aircraft wheel printing on prefabricated panels are shown in table 2, includes 8 critical load position conditions. Figure 3 shows the schematic diagram of wheel printing on critical load position of case Z-4, the other cases are similar.

Table 2. Analysis of critical load condition.

Case	Action side (corner / midspan)	Action side (tenon / groove)	Relationship between wheel printing and panel side (parallel / vertical)	Surface load (MPa)	Note
Z-1	Corner	Groove	Parallel	1.47	Same as Z-6
Z-2	Corner	Groove	Vertical	1.47	Same as Z-5
Z-3	Midspan	Groove	Parallel	1.47	-
Z-4	Midspan	Groove	Vertical	1.47	-
Z-5	Corner	Tenon	Parallel	1.47	Same as Z-2
Z-6	Corner	Tenon	Vertical	1.47	Same as Z-1
Z-7	Midspan	Tenon	Parallel	1.47	-
Z-8	Midspan	Tenon	Vertical	1.47	-

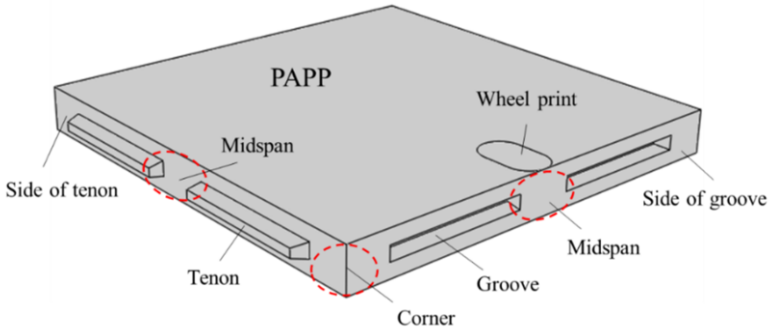

Figure 3. Schematic diagram of wheel printing on critical load position of case Z-4.

3. Result Analysis

In this section, the extreme nephogram is given by taking the case of Z-2 as examples. Table 3 shows the results of the critical load level under all cases.

Table 3. Action results of critical load.

Case	Concrete panel					Prestressed rebar			Rebar in panel			Stratum	
	MA (MPa)	MI (MPa)	MS (mm)	MO (10^{-3} mm)	MC (10^{-3} mm)	MA (MPa)	MI (MPa)	MS (mm)	MA (Mpa)	MI (MPa)	MS (mm)	MS (mm)	Same as
Z-1	1.59	3.65	0.31	5.34	4.64	2.56	0.80	0.30	10.28	6.08	0.30	0.30	Z-6
Z-2	2.22	2.23	0.30	5.30	4.74	2.16	0.97	0.30	8.11	6.54	0.30	0.30	Z-5
Z-3	1.37	1.83	0.30	1.12	2.24	1.92	0.89	0.29	5.94	5.03	0.29	0.29	-
Z-4	1.34	1.68	0.29	1.11	2.00	1.70	0.82	0.29	5.53	5.52	0.29	0.28	-
Z-5	2.22	2.23	0.30	5.30	4.74	2.16	0.97	0.30	8.11	6.54	0.30	0.30	Z-2
Z-6	1.59	3.65	0.31	5.34	4.64	2.56	0.80	0.30	10.28	6.08	0.30	0.30	Z-1
Z-7	1.45	1.91	0.30	1.51	2.04	3.13	1.34	0.29	6.15	5.24	0.29	0.29	-
Z-8	1.41	1.84	0.29	1.57	1.85	2.72	1.30	0.29	5.90	5.13	0.29	0.29	-
Limit	2.39	26.8	-	-		300	300	-	300	300	-	-	-
Result	Satisfy	Satisfy	Small	Small	Small	Satisfy	Satisfy	Small	Satisfy	Satisfy	Small	Small	-

Note: MA-Maximum principal stress, MI-Minimum principal stress, MS-Maximum settlement, MO-Maximum opening of contact surface, MC-Maximum compression of contact surface.

According to the mechanical properties of the model material, the maximum principal stress (MAPS) can be used to judge the tensile condition of the model structure, and the minimum principal stress (MIPS) can be used to judge the compression condition of the model structure. Figure 4 shows the nephogram of the extreme value of the principal stress of the prefabricated panel. It can be seen from table 3: the ultimate load position of prefabricated panel is Z-2/5, the MAPS is 2.22 MPa, and the MIPS is 2.23 MPa, it can be seen that the extreme value of the principal stress of the prefabricated panel meets the limit value of the current specification. In combination with the characteristics of excellent compressive performance and poor tensile performance of concrete, the control item of the prefabricated panel is the maximum principal stress.

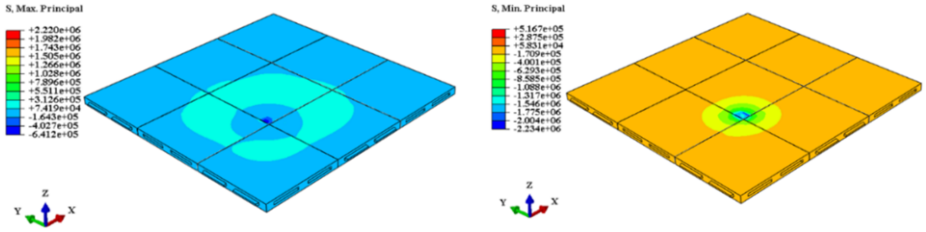

(a) Z-2 MAPS 2.22 (b) Z-2 MIPS 2.23

Figure 4. Z-2 extreme values of principal stress of prefabricated panel (MPa).

Figure 5 shows the nephogram of the principal stress extreme value of the prestressed rebar. The ultimate load position of prestressed rebar under single wheel action is Z-7 case, the MAPS is 3.13 MPa, and the MIPS is 1.34 MPa; the extreme value of the principal stress of the prestressed rebar is small, which is far less than the limit value of the current specification. The prestressed rebar still has large design redundancy under the action of single wheel limit load positions.

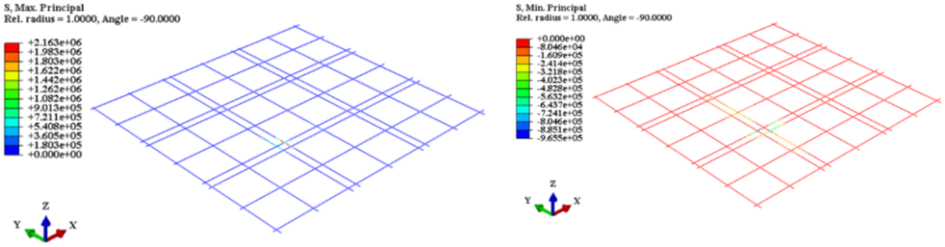

(a) MAPS 2.16 (b) MIPS 0.97

Figure 5. Z-2 principal stress extremum of prestressed rebar (MPa).

Figure 6 shows the nephogram of the principal stress extreme value of the steel rebar in the panel. It can be seen from table 3: the ultimate load position of the rebar in the panel is under the case of Z-1/6, the MAPS is 10.28 MPa, and the compression is under the case of Z-2/5, and the MIPS is 6.54 MPa; the extreme value of the principal

stress of the rebar in the panel is small, far less than the limit value of the current specification. The rebar in the panel still has large design redundancy under the action of single wheel limit loads.

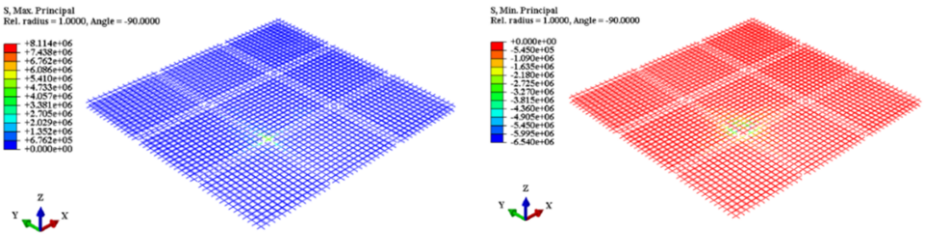

(a) Z-2 MAPS 8.11 (b) Z-2 MIPS 6.54

Figure 6. Z-2 extreme values of principal stress of rebar in panel (MPa).

Figure 7 shows the extreme nephogram of deformation (settlement) under the condition of ultimate load level. It can be seen from table 3: the maximum settlement of ultimate load level of prefabricated slab under the action of single wheel is 0.31 mm under the conditions of Z-1/6. The maximum settlement of prestressed rebar is 0.30 mm under Z-1/2/5/6 working conditions. The maximum settlement of rebar in the slab is 0.30 mm under Z-1/2/5/6 working conditions. The maximum settlement of stratum is 0.30 mm under Z-1/2/5/6 working conditions. In conclusion, the settlement of the new prestressed PAPP structure system is small and has excellent settlement resistance performance.

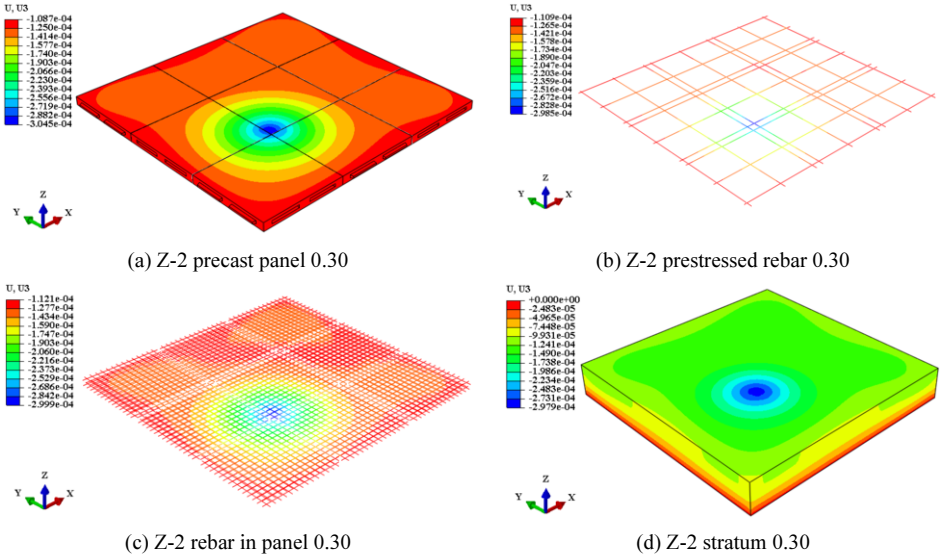

(a) Z-2 precast panel 0.30 (b) Z-2 prestressed rebar 0.30

(c) Z-2 rebar in panel 0.30 (d) Z-2 stratum 0.30

Figure 7. Extreme values of deformation (settlement) under limit load position condition (mm).

The biggest difference between the fabricated pavement and the cast-in-place pavement is that there are panel-panel joints and panel-stratum joint. The joint opening and compression deformation are important control indexes for evaluating the

structural system. The COPEN function of ABAQUS software can be used to check the opening and compression deformation of the contact surface under the load, so as to judge the deformation of the joint. Figure 8 shows the extreme values of contact surface opening and compression. It can be seen from table 3 that the maximum opening of panel-panel joints and panel-stratum joint under single wheel action occurs in Z-1/6 case, which is 5.34×10^{-3} mm.

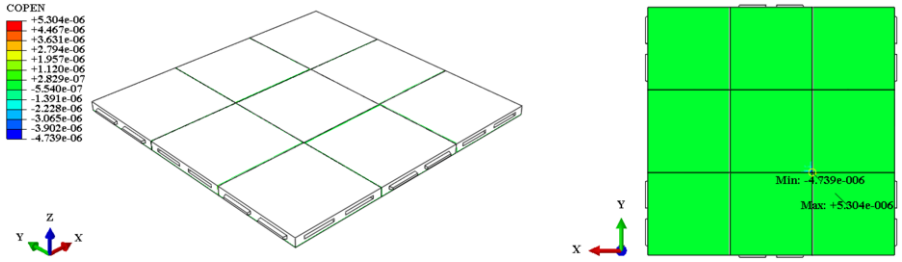

Figure 8. The maximum opening of Z-2 contact surface is 5.30 and the maximum compression is 4.74 (unit: 10^{-3} mm).

To sum up, it can be seen from the analysis and comparison of the influence range, control factors and bearing performance of single wheel cases: ① the calculation results of single wheel limit load positions show that the most unfavorable limit load position is the condition that the panel corner, side face of the panel are tenon and groove, and the wheel printing is perpendicular to the side face; ② the influence radius of the most unfavorable limit load position of single wheel (Z-2/5) is less than 0.5 R, affecting 8 panels around; ③ the design of the connection of the prestressed rebar and the tenon and groove structure between the panel and the panel has a better function of spreading the concentrated load of a single panel to the surrounding adjacent panels in a circular manner, and being uniformly and jointly carried by the adjacent panels, highlighting the mechanical and bearing advantages of the connection of the prestressed rebar and the tenon and groove under the action of multiple wheels of the single panel; ④ the mechanical properties of the new prestressed tenon and groove connection PAPP meet the requirements of the current specifications and have excellent mechanical bearing performance.

4. Conclusions

In this paper, a 3D-FEM is established for the new type of prestressed tenon and groove connection PAPP structure, and the numerical simulation analysis of the critical load position of single wheel under multiple cases is carried out. Study the mechanics, deformation and joint deformation performant, and the following understandings are obtained:

(1) The calculation results of single wheel limit load positions show that the most unfavorable limit load position is the condition that the edge corner and side face of the panel are tenon and groove, and the wheel printing is perpendicular to the side face. The influence radius of the most unfavorable limit load position of single wheel (Z-2/5) is less than 0.5 R, affecting 8 panels around.

(2) The connection design of prestressed rebar and tenon and groove structure between panel and panel has a good function of spreading the concentrated load of a single panel to the surrounding adjacent panels in a circular manner and uniformly bearing by the adjacent panels.

(3) The mechanical properties of the new prestressed tenon and groove connection PAPP meet the requirements of the current specifications and have excellent mechanical bearing properties.

Credit Author Statement

Peng Ding: Conceptualization, Methodology, Formal analysis, Investigation, Writing – original draft. Zhiguo Liu: Investigation, Writing – review & editing, Funding acquisition. Menglin Li: Conceptualization, Methodology, Supervision. Ran Zhou: Data review, Writing, Wenzhan Ji: Methodology, Formal analysis. Mengmeng Zhang: Numerical simulation analysis.

Declaration of Competing Interest

We declare that we have no competing financial interests or personal relationships that could appeared to influence the work described in this paper.

Acknowledgments

The authors gratefully acknowledgement the financial support provided by the CCSTC Science and Technology R & D Plan (No. ZJKJ-2021-3), CSCEC Science and Technology Innovation Platform (CSCEC-PT-005).

References

[1] Sapozhnikov N & Rollings RS. Soviet precast prestressed construction for airfields. In: Federal Aviation Administration, editor. Proceedings of the FAA Worldwide Airport Technology Transfer Conference, Atlantic City, NJ. 2007. p. 1-11.

[2] Tayabji S, Dan Y, & Neeraj B. Precast Concrete Pavement Technology. SHRP2, US Department of Transportation, Washington, USA. 2013.

[3] Ashtiani RS, Jackson CJ, Saeed A & Hammons MI. Pre-cast concrete panels for contingency rigid airfield pavement damage repairs. Report AFRL-RXTY-TR-2010-0095. Air Force Research Laboratory, Materials and Manufacturing Directorate, Panama City, FL. 2010.

[4] Priddy LP, Bly PG, Jackson CJ & Flintsch GW. Full-scale field testing of precast portland cement concrete panel airfield pavement repairs. International Journal of Pavement Engineering. 2014; 15(9-10):840-853.

[5] Rollings RS & Chou YT. Precast concrete pavements. Miscellaneous Paper GL-81-10. U.S. Army Engineer Waterways Experiment Station, Vicksburg, MS. 1981.

[6] Sander TC & Roesler JR. Case study: runway 12L-30R keel section rehabilitation, Lambert — St. Louis International Airport. In: Al-Qadi IL, editor. Proceedings of the Airfield and Highway Pavements Specialty Conference (ASCE), 2006 Apr 30 - May 3; Atlanta, GA: ASCE Press; p. 872-884.

[7] Farrington R, Rovesti WC, Steiner D & Switzer WJ. Overnight concrete pavement replacement using a precast panel and expanding polymer positioning technique—Washington Dulles International Airport case study. In: Karakouzian M, editor. Proceedings of the Airfield Pavements Specialty Conference

(ASCE), 2003 Sep 21-24; Las Vegas, NV. ASCE Press; p. 13-28.
[8] Switzer WJ, Fischer A, Fuselier GK, Smith PJ & Verfuss W. Overnight pavement replacement using precast panels and conventional subgrade material, Washington Dulles International Airport case study. In: Karakouzian M, editor. Proceedings of the Airfield Pavements Specialty Conference (ASCE), 2003 Sep 21-24; Las Vegas, NV. ASCE Press; p. 259-278.
[9] Chen YS, Murrell SD. & Larrazabal E. Precast concrete (PC) pavement tests on taxiway D-D at LaGuardia Airport. In: Karakouzian M, editor. Proceedings of the Airfield Pavements Specialty Conference (ASCE), 2003 Sep 21-24; Las Vegas, NV. ASCE Press; p. 447-483.
[10] Karmacharya A, Gamarra J & Chao SH. (2019). Use of Ultra-high-performance fiber-reinforced concrete (UHP-FRC) for fast and sustainable repair of rigid pavements. In: Al-Qadi I, Ozer H, Loizos A, Murrell A, editors. Proceedings of the International Airfield and Highway Pavements Conference (ASCE), 2019 Jul 21-24; Chicago, IL. ASCE Press; p. 273-285.
[11] Senseney CT, Smith PJ & Snyder MB. Precast concrete paving repairs at Vancouver International Airport. Transportation Research Record Journal of the Transportation Research Board. 2021; 2675(9), 439-448.
[12] Ling JM, Liu W & Zhao HD. Mechanical responses of rigid airport pavement to multiple-gear military aircraft loadings. China Civil Engineering Journal. 2007; 40(4), 60-65.
[13] Qu B, Weng XZW, Zhang J, Mei JJM, Guo TX, Li RF & An SH. Analysis on the deflection and load transfer capacity of a prefabricated airport prestressed concrete pavement. Construction and Building Materials. 2017; 157, 449-458.
[14] Guo TX, Weng XZ, Qu B, Zhang CX, Li YZ, Liu JZ & Cui T. Full-scale investigation of thermal deformation and load transfer performance of prefabricated prestressed concrete pavement for airports. Journal of Transportation Engineering Part B-Pavements. 2020; 146(3).